Catalysis Today 177 (2011) 31–38

Contents lists available at ScienceDirect

Catalysis Today

journal homepage: www.elsevier.com/locate/cattod

Formation of oxygen active species in Ag-modified CeO_2 catalyst for soot oxidation: A DFT study

Gloria Preda, Gianfranco Pacchioni*

Dipartimento di Scienza dei Materiali, Università di Milano-Bicocca, Via R. Cozzi, 53-20125 Milano, Italy

ARTICLE INFO

Article history:
Received 26 January 2011
Received in revised form 15 March 2011
Accepted 1 April 2011
Available online 24 May 2011

Keywords:
Ceria
DFT calculations
Silver clusters
Oxygen vacancy

ABSTRACT

In this paper, we analyze from a theoretical point of view, based on the existing literature and on specific first principles DFT calculations, some aspects of the reactivity of Ag-modified CeO_2 surfaces used for soot combustion in particulate diesel filters. We have considered various species adsorbed and coadsorbed on the $CeO_2(1\,1\,1)$ stoichiometric and reduced surface: O_2 molecules, small carbon clusters, isolated Ag atoms and small Ag clusters. Carbonaceous species react with the ceria surface with formation of oxygenated carbon fragments and subsequent formation of reduced ceria but the mechanism which occurs to replenish the oxygen content of the oxide catalyst is still unclear. The formation of peroxo and superoxo species is discussed. The role of silver in modifying the properties of $CeO_2(1\,1\,1)$ has also been considered. Ag atoms and Ag_5 clusters act as donor species, become oxidized and donate the valence electron to the oxide with formation of reduced Ce^{3+} ions. A charge transfer in the opposite direction occurs when Ag atoms are bound to O vacancies. In the second case, we notice that in the presence of gas-phase oxygen the formation of superoxo species can be mediated by small Ag particles. However, the stronger affinity for oxygen of the vacancy compared to Ag always leads as a final result to filling the cavity by ambient oxygen.

1. Introduction

CeO_2-based catalysts are receiving an increasing attention due to their unique properties for application in automotive car exhausts treatment. Three-way catalysts (TWC) used in gasoline-powered engines are designed to eliminate hydrocarbons, CO, and NO_x; most TWC formulations combine CeO_2-based materials with noble metal nanoparticles. In the last years, however, diesel-powered engines have considerably increased their worldwide usage (nowadays about 60% of all commercial vans are equipped with diesel engines) and their exhausts abatement poses a series of problems to meet legislation requirements [1]. The most used technology to reduce diesel exhausts is based on filtering systems consisting of a trap capable to collect the particulate, mostly composed by carbon soot. Once the particulate has been collected, it must be burned off in order to regenerate the filter, usually a ceramic wall-flow monolith. Diesel particulate spontaneously burns in air at temperatures of about 500–600 °C, a temperature not reached in typical diesel vehicles. If an excess of soot is collected on the filter the gas exhaust cannot diffuse and the pressure and the temperature can increase considerably, and eventually result in the melting of the filter. A key technological issue is therefore the reduction of the combustion temperature of the soot. One of the methods currently adopted is the use of a CeO_2-based catalyst added to the filter, since several reports show that CeO_2-based oxides have excellent activity for soot oxidation at relatively low temperatures [1].

Two effects play a very important role in the formulation of the catalyst. One is the intensity of the contact between the soot and the catalyst. In principle, one can have a "loose" or a "tight" contact, where this second case leads to much better performances [2,3]. In evaluating the efficiency of a modified catalyst in soot combustion the exact level of contact is an essential parameter. The other aspect is that several studies indicate an improved activity of the catalyst when ceria is mixed with other oxides or simply doped with transition metal or lanthanide atoms [4–9]. The role of these dopants can be of different type. For instance, it has been suggested that La^{3+} ions have the effect of stabilizing ceria particles with larger surface area and to raise the sintering temperature of the particles [7]. Since ceria is an oxygen storage catalyst, it is also possible that these dopants increase the mobility of oxygen species or facilitate the redox mechanisms associated to the oxygen release/adsorption [10].

Another aspect which has been investigated is the role of transition metal particles on the activity of CeO_2 in soot combustion [5,11,12]. This is closely related to the efficiency of soot combustion but also to the removal of other contaminants like CO and NO_x. It is generally assumed that the soot oxidation proceeds via

---

* Corresponding author.
E-mail address: gianfranco.pacchioni@mater.unimib.it (G. Pacchioni).

0920-5861/$ – see front matter © 2011 Elsevier B.V. All rights reserved.
doi:10.1016/j.cattod.2011.04.036

a Mars–Van Krevelen mechanism where the carbon particles are oxidized by lattice oxygen with formation of oxygen vacancies and consequent reduction of CeO_2 (Ce^{4+}) to CeO_{2-x} (Ce^{3+}) [5,6]. Soot oxidation experiments performed in the presence of $^{18}O_2$ have shown that the gas-phase labelled oxygen replaces lattice oxygen creating new highly active nonlabelled oxygen species [6]. In this process, the role of a transition metal like Pt is probably that to facilitate the dissociation of the oxygen molecules coming from the gas-phase, thus lowering the energy demand for a crucial step in the whole catalytic cycle.

From this brief introduction, it is clear that despite a considerable amount of data acquired on this system, some microscopic aspects of the mechanism of the oxidative process are still unclear. Nevertheless, some firm points have been established in the literature, like the formation of paramagnetic O_2^- superoxo species shown by EPR and infra-red [4,13,14] or the detection of diamagnetic O_2^{2-} peroxo species by Raman spectroscopy [15–17] when reduced CeO_{2-x} samples are exposed to oxygen. It has been suggested that these are the precursor surface species which initiate the soot oxidation. On the other hand, other mechanisms have been proposed like the involvement of lattice oxygen or of oxygen species which form directly at the soot/catalyst interface [10].

Due to its intrinsic importance in catalytic processes, the study of CeO_2, CeO_{2-x}, and Ce_2O_3 surfaces has attracted a large interest from the theoretical community in the last years [18–24]. The theoretical treatment of reduced CeO_2 presents several problems and difficulties. These methodological problems are added to the intrinsic complexity of the function of the catalyst, thus making the entire problem extremely challenging from a theoretical point of view. One of the problems connected to the use of electronic structure methods for the description of reduced ceria is that standard density functional theory (DFT) fails in describing the localized nature of the Ce 4f states [19,25,26]. This can be partly removed by using hybrid functionals [20,27] or the so called DFT + U approach [25,26,28] where the standard DFT energy functional is augmented by an on-site Hubbard-like interaction that depends on the difference $U_{\text{eff}} = U - J$, where U and J represent the energy cost of adding an extra electron at a particular site and the screened exchange energy, respectively. Since U can be considered as a parameter, the cost of removing one oxygen atom from a regular CeO_2 surface (i.e. the formation energy of an oxygen vacancy) strongly oscillates as a function of the theoretical method adopted [29,30]. Other problems in the treatment of CeO_2 arise from the fact that the change in oxidation state of the Ce ion from 4+ to 3+ results in a change of lattice parameter which is not treated accurately enough at all levels of theory [31]. Recently, it has been suggested that the DFT approach in the local density approximation (LDA) is better suited to describe the geometrical structure of the material, while the more advanced generalized gradient approximation (GGA) should be used in order to obtain more reliable energy differences [31]. A combined use of LDA for geometry and GGA for energy has thus been proposed [31], and is adopted here.

2. Computational methods

Spin polarized DFT calculations have been carried out to study the interaction between Ag atoms and clusters and O_2 molecules and the $CeO_2(1\,1\,1)$ surface. This is the most stable surface exposed by ceria crystallites. The calculations have been carried out with the Vienna ab initio simulation package (VASP) [32,33] using a plane wave basis set and the projector augmented wave (PAW) method [34] to describe the interaction between the valence electrons and the atomic cores. The valence electron density is defined by the twelve ($5s^2 5p^6 6s^2 5d^1 4f^1$) electrons of each Ce atom, the six ($2s^2 2p^4$) electrons of each O atom, and the eleven ($5s^1 4d^{10}$) electrons of Ag. The plane-wave expansion includes all plane waves with kinetic energy smaller than a cutoff of 415 eV. The LDA + U or GGA + U approaches [35–37] were chosen to account for exchange and correlation. The LDA and GGA parts of these functionals are those of Vosko et al. [38] (VWN) and Perdew–Wang [39,40] (PW91), respectively. In the LDA + U (and GGA + U) method part of the self-interaction energy is corrected by explicit inclusion of a Hubbard like U_{eff} term for the 4f electrons penalizing partial occupancy of this atomic level. In the present work, we used the formalism of Dudarev et al. [41]. Numerical integration in the reciprocal space was carried out using a $2 \times 2 \times 1$ Monkhorst–Pack special k-points grid [42]. A Methfessel–Paxton smearing width $\sigma = 0.2$ eV was applied to help to converge the electronic density [43].

Geometry optimization has been performed within the LDA + U with $U_{\text{eff}} = 5$ eV scheme because it provides a lattice parameter which is close to experiment [19,28]; magnetic moments and Bader charges [44,45] have been obtained at the same level of theory whereas energies were calculated at the GGA + U level with $U_{\text{eff}} = 3$ eV (for a detailed discussion of the motivation of this choice see Ref. [28]). This choice allows one to properly describe localization in bulk Ce_2O_3 as well as in ceria nanoparticles containing both Ce^{3+} and Ce^{4+} atoms.

To model the O-terminated $CeO_2(1\,1\,1)$ surface 2×2 (Ce_8O_{16}) or 3×3 ($Ce_{18}O_{36}$) supercells with 6 layers have been used keeping the three bottom layers fixed and relaxing the uppermost ones. The slab model was cut from the bulk cubic ($Fm3m$) CaF_2-like structure using the optimized lattice parameter a_0 of 5.40 Å, in excellent agreement with experimental $a_0 = 5.41$ Å. The supercell includes a vacuum of 12 Å which is large enough to avoid interaction between the slabs obtained after replication in the three space dimensions.

3. Results and discussion

3.1. $CeO_2(1\,1\,1)$ and $CeO_{2-x}(1\,1\,1)$

The electronic structure of a stoichiometric $CeO_2(1\,1\,1)$ surface, as deduced from the corresponding density of states (DOS, not reported) shows that the valence band, about 4 eV wide, is mainly formed by O 2p levels, and is separated by a gap of about 5.1 eV from the conduction band which originates from the Ce 5d orbitals. For comparison, the experimental band gap is 6 eV [46]. In CeO_2 all cerium-centered valence states are empty, but the very localized 4f states lie in the gap at 2.1 eV above the top of the valence band (3 eV the experiment). The removal of a surface oxygen and the consequent formation of an oxygen vacancy is a relevant process for the catalytic properties of CeO_2. According to our calculations, the vacancy formation energy, computed with respect to (1/2) O_2, is 3.54 eV (6.62 eV with respect to atomic O). This is in line with other values reported in the literature [29], also considering the intrinsic difficulty to compute this quantity in reducible oxides [30]. This is an important quantity since it has been proposed that the soot oxidation occurs at the expense of lattice oxygens.

The removal of one oxygen atom corresponds to a reduction of the system and in fact two electrons are found in localized 4f states on two surface Ce ions which change their configuration from $Ce^{4+}(4f^0)$ to $Ce^{3+}(4f^1)$[46]. This change in atomic configuration is accompanied by the appearance in the energy gap of the material of defect states associated to the localized 4f electrons; these states are located at about 1.4 eV from the top of the valence band. The strong localization of the 4f electron is demonstrated, for instance, by a plot of the spin density of the system (not shown) indicating the presence of an unpaired electron on two specific Ce atoms of the surface, one nearest neighbor to the missing oxygen and one on a Ce of the upper layer. All these features are consistent with other studies reported in the literature [19,22,25], and for this reason are no longer discussed. Furthermore, recent studies have shown that there is a distribution of Ce sites where the localization of the electrons associated to the oxygen vacancy can take place so that multiple structures exist with formally the same electronic configuration but with similar total energies (the differences are typically of 0.1 eV or less and all states are within 0.5 eV from the ground state) [47,48]. Since electron transport in these materials occurs by hopping, the existence of several states nearly degenerate in energy suggests a relatively easy electron mobility at finite temperatures. The activation energy for polaron electron transport in the bulk is indeed quite low, about 0.4 eV [49]. This may be important in view of the mechanism which is at the basis of the formation of superoxo O_2^- and peroxo O_2^{2-} ions.

3.2. O_2 adsorption on $CeO_2(1\,1\,1)$ and $CeO_{2-x}(1\,1\,1)$

The first step to consider in the catalytic oxidation of soot is the mechanism of interaction of gas-phase oxygen with the ceria surface. In fact, a key step in the proposed oxidation mechanism consists in the regeneration of the stoichiometry of the ceria particle after lattice oxygens have been transferred to the carbon particles. However, according to the present calculations, and in agreement with previous studies, the oxygen molecule is, at most, physisorbed on the stoichiometric $CeO_2(1\,1\,1)$ surface [50,51], giving rise to a very weak interaction dominated by dispersion forces (not well described in DFT). The adsorption energy, <0.1 eV, is so low that adsorption is possible only at very low temperatures and the O–O distance is the same as in gas-phase, 1.22 Å. In fact, Raman spectra of adsorbed molecular O_2 show the typical absorption band at 1551 cm^{-1} only below 150 K [15]. This means that oxygen can react only with defect sites at the ceria surface, like low-coordinated atoms at step edges, oxygen vacancies, or their aggregates.

Indeed, a completely different situation is found when the O_2 molecule is adsorbed on a O vacancy site. Here the interaction is strong, 3.15 eV, and the molecule is adsorbed with one O atom filling the vacancy and the other pointing out from the surface. The O–O distance elongates from the gas-phase value, 1.222 Å, to 1.418 Å, typical of a peroxo group. The O–O axis is tilted and forms an angle of about 50° from the surface normal. While the initial defective surface contains two unpaired electrons localized on two Ce^{3+} ions, the adsorption of an O_2 molecule in its $^3\Sigma_g{}^-$ ground state results in a complete magnetic quenching and the surface complex is diamagnetic. This result, combined with the long O–O bond and the analysis of the atomic charges according to the Bader approach (−0.705 and −0.531 e), points towards the formation of a peroxo group at the $CeO_2(1\,1\,1)$ surface. The new surface oxygen species can be seen as derived from the adsorption of atomic oxygen in its ^3P ground state on-top of an O atom of the regular $CeO_2(1\,1\,1)$ surface. The energy required to dissociate the peroxo group and release a gas-phase O atom is 2.70 eV (if computed with respect to $(1/2)\,O_2$ the process is slightly exothermic, −0.40 eV). This energy is quite relevant in the context of oxidative processes taking place on the surface, as it will be discussed below, because it is considerably smaller than the energy required to remove an oxygen from a regular site (6.62 eV). Peroxo groups are thus source of more reactive oxygen.

The formation of a peroxo species is in line with what reported by other authors who also found the spontaneous formation of O_2^{2-} when molecular oxygen interacts with a defective ceria surface [50–52]. The presence of these groups has also been confirmed experimentally by Raman spectroscopy since typical bands in the 830–870 cm^{-1} region arise when these groups are formed [15,16]. Experimentally, also the presence of paramagnetic superoxo O_2^- species has been reported by several authors. The proof of the formation of such species comes from EPR spectroscopy [13] but also from the analysis of Raman spectra since a typical band around 1120 cm^{-1} appears in correspondence to the formation of superoxo groups [15,16].

In principle, O_2^- species could form by O_2 adsorption on regular sites of a reduced CeO_{2-x} surface followed by an electron transfer from one Ce^{3+} $4f^1$ state to the $2\pi^*$ MOs of the adsorbed O_2 molecule. This is indeed the typical process occurring on other reduced oxides like TiO_2 where oxygen adsorbed on the non-defective surface acts as an electron scavenger which traps electrons from the reduced Ti^{3+} ions of the bulk [53,54]. However, attempts to verify this hypothesis computationally failed in the case of CeO_{2-x}. The adsorption of an O_2 molecule on a *regular site* of CeO_{2-x} resulted only in weak adsorption and no charge transfer. The unpaired electrons remain localized on the Ce^{3+} ions even when these are at the surface. This result suggests that, differently from other semiconducting oxides, in CeO_2 the 4f levels are deeper in energy then the O_2 $2\pi^*$ levels, so that a charge transfer between these two entities can only occur when these species are in close contact (e.g. for a low-coordinated Ce^{3+} ion). We also checked that this conclusion is not due to limitations or assumptions related to the computational approach adopted since these in principle could affect the relative positions of the Ce 4f and O_2 $2\pi^*$ levels (in particular the 4f levels could be artificially stabilized by the choice of the U parameter). However, the same result has been obtained at the standard GGA–DFT level, indicating that it is not related to the level of treatment.

In a recent study Conesa has suggested that superoxo O_2^- species form when O_2 interacts directly with a "single electron" oxygen vacancy [52]. This has been obtained by replacing a tetravalent Ce^{4+} ion by a trivalent La^{3+} ion, thus leaving only one Ce^{3+} associated to an O vacancy. Of course, in this case only one electron can be transferred to adsorbed O_2 and a superoxo, and not a peroxo, is formed. What remains to be clarified is how "single electron" oxygen vacancies can be formed on a real ceria surface. A possibility is that, due to the electron mobility, in some cases only one electron remains in the vicinity of the vacancy so that only a single electron transfer can occur.

There is a more likely explanation for the formation of superoxo anions. Recently, we have shown that O_2^- species can form by direct interaction of molecular oxygen with low-coordinated Ce ions. These are present at extended defects of the ceria surface (edge, steps, dislocations, etc. [22]) and are abundant on ceria nanoparticles since Ce^{3+} cations tend to be located at low coordinated sites of CeO_{2-x} reduced particles [23]. O_2 molecules interact strongly (with a binding energy of more than 1 eV) with the exposed Ce^{3+} ions [55]. The interaction leads to a charge transfer from Ce 4f states to the $\pi_g{}^*$ MO of O_2, resulting in fully oxidized Ce^{4+} ion and O_2^- superoxide species. The O_2 molecule binds preferentially in a side-one mode, with the end-on isomer clearly less favorable. Furthermore, the ground state structure of the end-on isomer is linear and not bent, as often assumed in the literature [55]. Recently, a direct correlation between size of ceria nanocrystals and oxygen activation has been demonstrated experimentally [56], consistent with the idea that superoxo species form on low-coordinated sites.

In summary, the classical model of an oxygen vacancy at the surface of reduced ceria explains the formation of diamagnetic peroxo groups, while the presence of Ce^{3+} ions at low-coordinated sites can be considered responsible for the formation of superoxo radical species. In both cases the O_2 molecule is activated and easier to dissociate in O atoms which can replenish the oxygen content of the ceria catalyst involved in soot oxidation.

3.3. Reactivity of oxygen surface species towards carbon soot

The formation of peroxo (or possibly superoxo) species at the CeO_2 surface is an important step in the catalytic cycle. If one

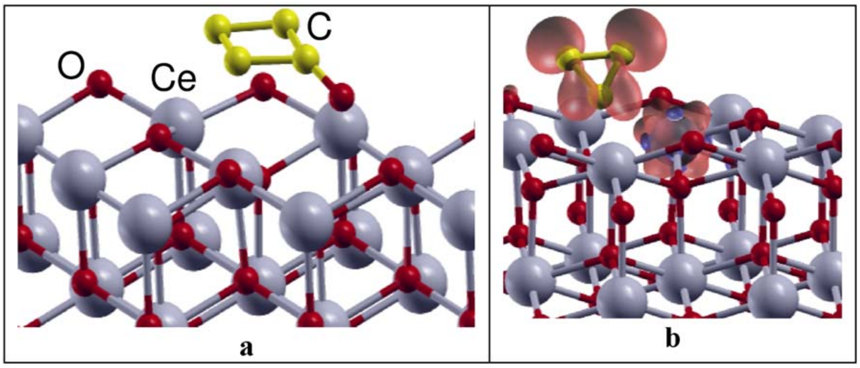

Fig. 1. (a) Structure of a C_4 cluster adsorbed on the $CeO_2(1\,1\,1)$ surface. (b) Structure of a C_3 cluster adsorbed on the $CeO_{2-x}(1\,1\,1)$ surface resulting from the desorption of a CO molecule. The figure shows also the spin density.

considers the oxidation of the carbon soot one can formulate two hypothesis. In the first one the carbon particle interacts directly with a peroxo group with transfer of one O atom:

$$C_n + CeO_{2+x}\,(\text{peroxo}) \rightarrow C_nO_x + CeO_2 \tag{1}$$

The other possibility is that one O atom of the peroxo group diffuses on the surface and reacts with the deposited carbon soot. This second mechanism, however, is only possible at elevated temperatures since the barrier for O diffusion on $CeO_2(1\,1\,1)$ has been estimated theoretically and is 1.4 eV [50]. Assuming a simple activated diffusion with a typical exponential prefactor of 10^{11}, a barrier of 1.4 eV corresponds to a diffusion temperature of about 300 °C (assuming a prefactor 10^{13} the diffusion temperature would be of about 200 °C). Thus, at the normal temperature where diesel antiparticulate filters operate, the mobility of surface oxygen is expected to contribute to the oxidation process.

We have estimated the energy changes associated to reaction (1) taking an infinite graphene sheet as a simplified model of typical aromatic hydrocarbons present in carbon soot. Reaction (1) leads to the formation of a graphene oxide where an O atom is bound to a graphene layer. The oxygen atom has been added in a bridge position over two C atoms and we found that reaction (1) is nearly thermoneutral, with a computed $\Delta E = +0.35$ eV, suggesting that the oxygen atoms of the peroxo group are potential candidates for the process.

If one compares the reactivity of the peroxo groups with that of the regular surface oxide anions of $CeO_2(1\,1\,1)$:

$$C_n + CeO_2 \rightarrow C_nO_x + CeO_{2-x}\,(\text{reduced}) \tag{2}$$

The difference with reaction (1) is very clear: reaction (2) is endothermic by 4.25 eV, due to the much higher cost of removing an oxygen atom from a regular site of the CeO_2 surface. Of course, not only the thermodynamics but also the kinetics of the process will be strongly affected by the formation of peroxo groups, as the barrier for the reaction is expected to be considerably lower.

Unfortunately, these computational results, showing the high reactivity of peroxo groups formed at the surface of ceria from a thermodynamic point of view, are not fully compatible with the experimental evidence based on isotopic labeling experiments which show that it is not the oxygen coming from the gas-phase which is incorporated into the oxidized products, but rather the oxygen coming from the ceria lattice [6]. Thus, the simplest idea that gas-phase O_2 reacts with defects like oxygen vacancies and generates “active” O species which are transferred to the organic substrate either directly or upon diffusion on the surface is not consistent with this specific result. This means that the gas-phase O_2 molecule must generate active oxygen species (e.g. via peroxo or superoxo formation) that further diffuse into the bulk of the oxide (or to other surface regions) in order to regenerate the original oxygen content. On the other side, active oxygen species can directly originate from the interaction of supported carbon particles and the lattice oxygen. In general, the formation of an interface between the carbon soot or other promoting materials and the ceria surface can considerably lower the cost for extracting oxygen atoms.

To study the reactivity of ceria with adsorbed carbon species we have considered a C_4 cluster on the surface of $CeO_2(1\,1\,1)$. C_4 was considered in its rhombic ground state structure [57]. The cluster interacts with the cluster plane parallel to the surface and a binding energy of 2.02 eV. The interaction leads to an outwards displacement of a surface O atom which forms a direct bond with one of the apical C atoms, Fig. 1a. The C–O distance, 1.27 Å, is typical of oxygenated hydrocarbon species. In the final structure, the O atom has been pulled out from the surface by about 0.7 Å, Fig. 1a, so that de facto an O vacancy has been created. This process occurs spontaneously, with no energy barrier, and leads to an oxygenated carbon fragment. The desorption of the C_4O unit, which results in the formation of an O vacancy on the surface, costs 1.03 eV. The other possibility is that what desorbs is a CO molecule, leaving on the surface a C_3 unit bound to an O vacancy according to the reaction:

$$C_4 + CeO_2 \rightarrow C_3/CeO_{2-x}\,(\text{reduced}) + CO \tag{3}$$

For the C_3 cluster adsorbed on an O vacancy of $CeO_2(1\,1\,1)$ we have found two isomers almost isoenergetic, both with triangular shape and one of the apical C atoms pointing towards the vacancy, Fig. 1b. The C_3/CeO_{2-x} complex and CO are only 0.7 eV less stable than the C_4 unit adsorbed on the non-defective surface. This means that in the presence of adsorbed hydrocarbon species, the formation of CO (or CO_2) by means of the surface O atoms of the ceria catalyst is an energetically accessible process that can occur at relatively low temperatures.

3.4. Ag/CeO_2 catalysts

In a recent paper Machida et al. [58] have reported that loading the ceria catalyst with Ag metal leads to an improved catalytic activity and a lower combustion temperature. In their experiments, CeO_2 has been mixed with various amounts of Ag, from a few percent to about 20% in weight. The results show a reduction of the combustion temperature from about 390 °C to about 340 °C for 10% Ag content. This change in activity has been tentatively explained with the fact that metallic silver can promote the formation of superoxo species [59,60]. In fact, the EPR signal associated to this species increases slightly when CeO_2 is loaded with metallic silver [58]. In another study Aneggi et al. [61] have shown that Ag/CeO_2 samples (prepared by impregnation of CeO_2 with an aqueous solution of $AgNO_3$ followed by calcination) contain Ag

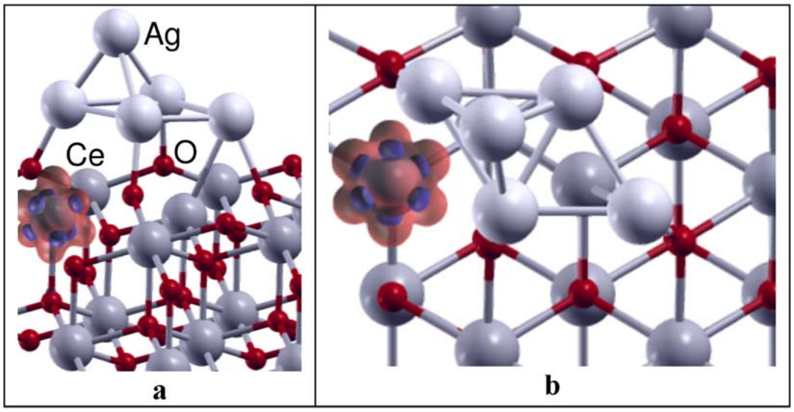

Fig. 2. Structure of Ag_5 cluster adsorbed on the $CeO_2(1\,1\,1)$ surface. (a) Side view; (b) top view. The figure shows also the spin density on a lattice Ce ion.

crystallites separated from the ceria particles by an Ag_2O phase. Also other authors have reported that ceria is able to maintain silver in a positive oxidation state [62]. In this respect, if one assumes that metallic silver is responsible for the promotion of O_2 to O_2^-, the interaction between ceria and silver is not ideal as it results in partial oxidation of silver.

An aspect which has not been considered in these studies is the possibility that diluted forms of silver (atom, clusters, nanoparticles) are formed during the synthesis and either adsorbed on the surface of the oxide or incorporated into the bulk. Due to their small dimensions, these species would not be detectable with normal electron microscopies. In a recent study on Au/Fe_2O_3 catalysts [63] it has been suggested, based on high resolution transmission electron microscopy with aberration correction, that the catalytic activity is due to less than 1% in weight of the deposited gold. This is present in the form of tiny clusters (less than 10 atoms) and even single gold atoms [63]. Therefore, nanosized Ag particles, Ag ions substituting for Ce, or even supported Ag atoms could act as promoters of the catalytic activity facilitating the oxygen adsorption and dissociation. Metiu and coworkers have demonstrated that the presence of Ag ions replacing Ce ions in the surface of $CeO_2(1\,1\,1)$ causes a considerable weakening of the Ce–O bond and a much lower formation energy of oxygen vacancies [64]. According to this model, if the Ag ions segregate towards the surface they facilitate oxidation mechanisms based on the Mars–Van Krevelen mechanism since the activation barrier for oxygen transfer is considerably reduced.

In this work, we have considered two other possibilities. We studied the interaction of an Ag atom and a Ag_5 cluster with the regular and defective surfaces of $CeO_2(1\,1\,1)$. From these model systems we hope to gain insight into the role of the CeO_2/Ag interface in promoting the soot combustion. The Ag atom has been adsorbed on various sites of the $CeO_2(1\,1\,1)$ regular surface, but only two sites appear to be stable. In one case Ag is above an O atom of the third layer and is bound to three O atoms of the first atomic layer; in the other case Ag_1 is directly on-top of an O atom of the first atomic layer. The first situation is preferred, and Ag is bound by 0.7 eV with respect to the gas-phase atom. In this site Ag forms three Ag–O bonds of 2.27 Å. Notice that the absolute value of the Ag binding energy should be taken with care since it has been shown that this can change significantly with the computational setup adopted [65]. However, what is common to all methods is the electronic structure of the system. In fact, in all sites Ag behaves as an electron donor with respect to CeO_2 with formation of an Ag^+ cation and a reduced Ce^{3+} ion:

$$Ag_1 + CeO_2 \rightarrow Ag_1{}^+/CeO_2{}^- \,(1\,Ce^{3+}) \qquad (4)$$

This is clearly shown (1) by the value of the Bader charge on Ag, +0.54 e, (2) by the spin density maps which indicate that the 5s electron of Ag is no longer present while an unpaired electron is localized on the 4f states of one Ce ion, and (3) by the DOS plots which show the appearance of a singly occupied 4f state in the band gap of the material. Thus, Ag atoms act as other promoters like alkali metals and result in the formation of reduced Ce^{3+} ions.

Also an Ag_5 cluster has been deposited on the $CeO_2(1\,1\,1)$ surface. In the gas-phase Ag_5 has a planar trapezium (2D) ground state structure; a trigonal bipyramid (3D) structure is 0.67 eV higher in energy. The Ag_5 cluster has a magnetic doublet ground state. We deposited the 3D Ag_5 cluster on the CeO_2 surface so that one triangular face is in direct contact with three O atoms of the surface and we fully reoptimized the structure. One of the Ag atoms in the cluster second layer moves towards the surface forming another bond with an O atom, Fig. 2. This clearly indicates that the strength of the Ag–O bond competes with that of the Ag–Ag bonds and that the cluster tends to wet the surface. Notice that we did not looked for other more stable isomers and that the structure reported in Fig. 2 is not necessarily the most stable isomer for Ag_5 on $CeO_2(1\,1\,1)$. On the other hand, it is representative of possible situations and reaction mechanisms associated to the presence of Ag clusters and small Ag particles at direct contact with the ceria surface.

The Ag_5 cluster is bound by 2.42 eV to the oxide surface (computed with respect to the bypiramidal trigonal isomer); this corresponds to an average bond strength of about 0.6 eV per Ag-O bond. As for a single Ag atom, also for Ag_5 we find a net charge transfer towards the oxide (the Bader charge on Ag_5 is +0.63 e). The cluster is ionized, and one electron is transferred to a surface Ce ion which changes oxidation state from Ce^{4+} to Ce^{3+}. However, while the Ag atoms at the interface are slightly oxidized (the average Bader charge is +0.14 e), the apical Ag atom keeps its metallic character (Bader charge +0.04 e). The O atoms at direct contact with Ag_5 relax outwards by about 0.15 Å in response to the presence of the metal cluster. In summary, Ag atoms or Ag nanoclusters deposited on a stoichiometric CeO_2 surface tend to become oxidized with consequent reduction of the Ce ions of the support. The next step has been to consider the same species adsorbed on an oxygen vacancy (interaction of reduced ceria with silver species).

An Ag atom binds rather strongly to an O vacancy at the $CeO_{2-x}(1\,1\,1)$ surface. The binding energy, 1.4 eV, is twice that found on the regular surface. The Ag atom is directly on-top of an O atom of the third layer and in direct contact with three Ce atoms around the vacancy. In the minimum geometry the Ag–Ce distances are of 3.11–3.21 Å. Since two Ce^{3+} $4f^1$ ions are associated to the vacancy and Ag has a $5s^1$ valence configuration, there is a total of three unpaired electrons. In the final structure, however, only one unpaired electron remains due to an electron transfer from one Ce^{3+}

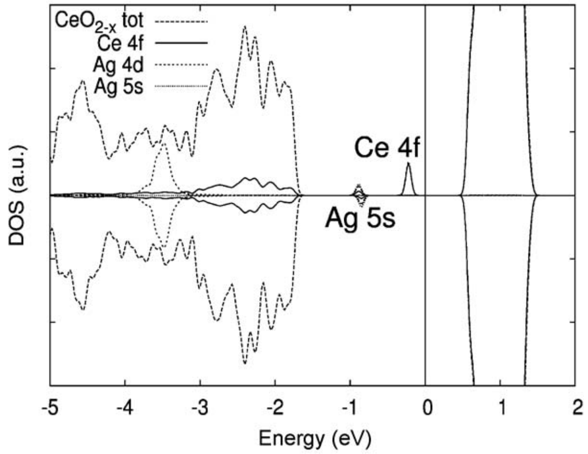

Fig. 3. Density of states of an Ag atom adsorbed on an O vacancy at the surface of the $CeO_{2-x}(1\,1\,1)$ surface.

ion to Ag_1 which formally becomes Ag^- ($5s^2$). The global process is:

$$Ag_1 + CeO_{2-x}\,(2\,Ce^{3+}) \rightarrow Ag_1{}^-/CeO_{2-x}{}^+\,(1\,Ce^{3+}) \qquad (5)$$

In the case of adsorption on an oxygen vacancy Ag acts as an oxidizing agent, more or less in the same way as molecular oxygen. The occurrence of the above process is confirmed, besides the spin density analysis, (1) by the Bader charges on Ag (−0.48 e) and (2) by the DOS curves which show the double occupancy of the Ag 5s level, Fig. 3.

At variance with the case of the stoichiometric surface, Ag_5 is not oxidized neither reduced when adsorbed on an O vacancy of $CeO_{2-x}(1\,1\,1)$. The Bader charges are between −0.20 and +0.28 e indicating partial charge redistribution within the cluster. The bonding, about 1.9 eV, is not stronger than on the non-defective surface but the cluster undergoes a substantial distortion due to the displacement of one of the Ag atoms towards a surface O atom (Fig. 4).

The next step has been considering the possibility that the deposition of an Ag_5 cluster on stoichiometric CeO_2 can result in the easier formation of an O vacancy and in the incorporation of O inside the metal cluster. The process considered is therefore:

$$Ag_5/CeO_2 \rightarrow Ag_5O/CeO_{2-x}\,(2\,Ce^{3+}) \qquad (6)$$

If the O atom is included inside the Ag_5 cluster, in an interstitial position of the Ag cage, the system is unstable and the O atom spontaneously moves towards the surface refilling the vacancy.

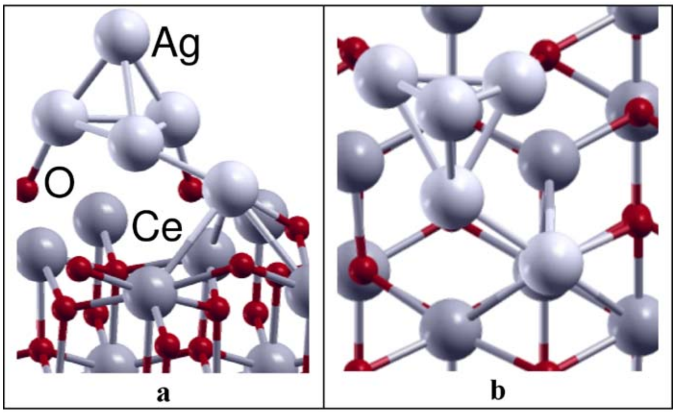

Fig. 4. Structure of Ag_5 adsorbed on the $CeO_{2-x}(1\,1\,1)$ surface. (a) Side view; (b) top view.

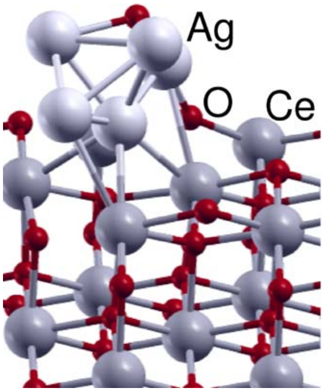

Fig. 5. Structure of Ag_5O adsorbed on the $CeO_{2-x}(1\,1\,1)$ surface. This has been obtained by displacing a surface O atom with formation of an oxidized Ag cluster and an O vacancy.

This result already indicates that the affinity of Ag for O is not particularly high. In fact, $\Delta H^\circ(Ag_2O)$, −31.1 kJ/mol, is much smaller than that CeO_2 ($\Delta H^\circ(CeO_2) = -1088.7$ kJ/mol). We found a structure where the O atom is bound to the top of the Ag_5 cluster, Fig. 5, but this corresponds only to a local minimum which is about 2.9 eV less stable than the reactants, see left side of Eq. (6). Thus, the presence of a small Ag cluster does not favor the formation of an O vacancy.

To conclude this section, we have found that Ag atoms or clusters tend to reduce the stoichiometric surface and transfer charge from the Ag 5s levels to the Ce ions of the oxide. An opposite effect occurs when the Ag atom is deposited on an O vacancy of CeO_{2-x}. However, there is no evidence that the presence of diluted forms of silver can induce the formation of O vacancies. What remains to be considered is the role of Ag atoms and clusters in the activation of molecular oxygen from the gas-phase.

3.5. *O_2 adsorption on Ag/CeO_2 catalysts*

In this section, we consider the interaction of O_2 molecules with adsorbed Ag atoms and clusters. We start from the case of a single Ag atom adsorbed on the stoichiometric $CeO_2(1\,1\,1)$ surface. We have seen that in this case Ag carries a positive charge. O_2 binds to the Ag^+ species by 0.45 eV forming a bent complex (r(Ag–O) = 2.116 Å, α(AgOO) = 111°). This is a considerably stronger bond than that of O_2 to the regular surface (see Section 3.2). Thus, an effect of diluted Ag atoms adsorbed on the ceria surface could be that to increase the sticking probability of the incoming O_2 molecules. However, there is no sign of activation of the O_2 molecule. The O–O bond distance, 1.251 Å, is only slightly elongated compared to gas-phase O_2. The spin remains localized on the reduced Ce ions (Ce^{3+}) and no oxidation of the support occurs. Thus, we have no sign of any particular promoting effect of Ag^+ ions adsorbed on the surface. We also considered another structure where the O_2 molecule interacts with the Ce^{3+} ion of the surface near the adsorbed Ag^+. This configuration has been considered in order to check possible bonding of O_2 at the interface between Ag_1 and CeO_2. The optimization leads to a weakly bound non-activated O_2 molecule, and no interaction with the Ag^+ ion is observed. Furthermore, no charge transfer occurs from the highly localized $4f^1$ state of Ce^{3+} to O_2. Thus, there is no direct beneficial effect from the presence of the Ag^+ ad-species.

The next case considered is that of O_2 adsorption on a Ag atom bound to an oxygen vacancy. We have seen that here the Ag adatom is negatively charged. We first placed the O_2 molecule on-top of the Ag atom, and reoptimized the structure. This results in a local minimum where the O_2 molecule is weakly bound to Ag, by

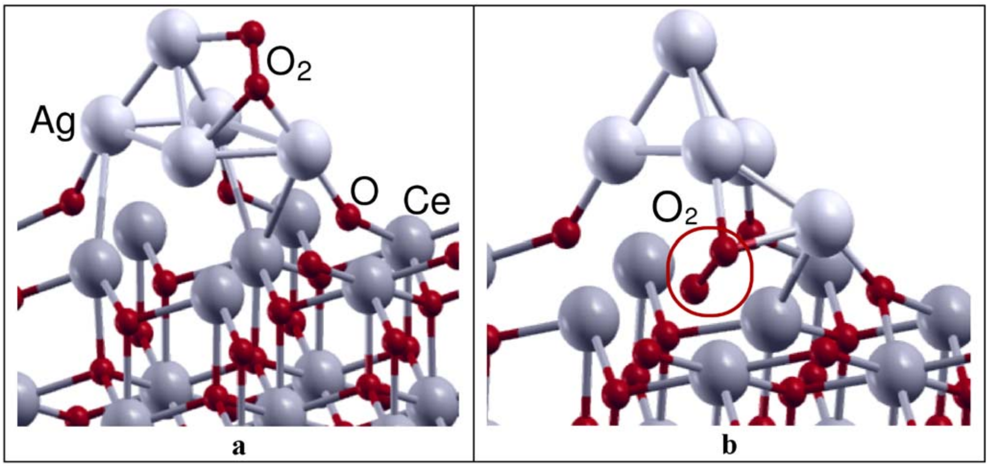

Fig. 6. Structure of O_2 adsorbed on Ag_5/CeO_{2-x}(1 1 1) surface complex. (a) Isomer where O_2 is above the Ag cluster and forms a superoxo species (less stable); (b) isomer where O_2 is below the Ag cluster and forms a peroxo group (more stable).

0.1 eV, forming a relatively long Ag–O bond, 2.239 Å, and an angle α(AgOO) = 119°. In this complex, the O_2 molecule is non-activated (r(O–O) = 1.250 Å) and the negative charge remains on Ag. However, a second more stable minimum exists where O_2 interacts with both Ag and the CeO_{2-x} surface (interface bonding). In this configuration, the O_2 molecule is strongly bound, by 2.06 eV, and induces a strong structural rearrangement. In fact, O_2 lies now parallel to the surface, and replaces the missing oxygen. This is not necessarily the lowest configuration; probably a barrier prevents the molecule from adsorbing with the molecular axis perpendicular to the surface, as for a typical peroxo species. The Ag atom is displaced from its original position, and shifted to a vicinal adsorption site where it is bound to three O atoms. Notice that this is the preferred position of Ag_1 on the regular surface. The O–O distance of the adsorbed O_2 molecule, 1.43 Å, is clearly indicative of the formation of a peroxo species, ${O_2}^{2-}$. Interestingly, the two extra electrons are not coming from the CeO_{2-x} substrate (there is still one Ce^{3+} ion in the supercell) but rather come from the Ag species which changes its oxidation state from −1 to +1. Stated differently, when the O_2 molecule interacts at the interface of Ag_1/CeO_{2-x} it takes the position of the Ag atom which is displaced to another adsorption site; a double charge transfer occurs from Ag to O_2 with formation of peroxo and Ag^+ species. The final result is that the Ag atom assumes the same position and oxidation state that it has on the stoichiometric surface (Ag^+). In this respect, the key role is not that of silver, but rather that of the oxygen vacancy which is the real source of electrons to reduce the oxygen molecule.

The last case considered is that where the O_2 molecule interacts with the Ag_5/CeO_{2-x} complex. The question we would like to answer is weather the simultaneous presence of the Ag_5 cluster and a reduced ceria surface results in an easier electron transfer to O_2 and in the activation of the molecule. To this end, we have adsorbed O_2 on top of the Ag_5 cluster and reoptimized the structure. We found a minimum where the O_2 molecule is bound to the Ag cluster, Fig. 6a, with the molecular axis almost normal to the surface. An electron transfer occurs from the Ag cluster to O_2 (not from the CeO_{2-x} support) with consequent formation of a superoxo radical (r(O–O) = 1.386 Å; Bader charges −0.45 and −0.37 e on the bottom and top O atoms, respectively, Fig. 6a). This structure (Fig. 6a), however, is about 1.8 eV less stable than a second structure where the O_2 molecule is below the Ag_5 unit, in direct interaction with the ceria surface, Fig. 6b. One of the O atoms fills the vacancy and the other is in direct contact with the Ag cluster; what is formed, however, is a peroxo group, as shown by the typical O–O distance of 1.46 Å and by the Bader charges, −0.71 and −0.60 e on the bottom and top O atoms. We have not investigated the barrier which separates the isomer where O_2 is adosorbed above from that below Ag_5 but at the temperatures at which soot oxidation occur there should be no problem in overcoming this barrier. This means that a small Ag cluster stabilized at an O vacancy can promote formation of superoxo species, but not in a catalytic way since it is likely that the O_2 molecule will diffuse below the cluster and saturate the vacancy. In this respect, also considering the other results obtained for O_2 interacting with supported species there is no unambiguous evidence that small silver clusters on ceria can have a special role in the activation of molecular oxygen.

4. Conclusions

In this paper, we have analyzed from a theoretical point of view, based on the existing literature and on specific first principles DFT calculations, some key aspects of the reactivity of Ag-modified CeO_2 surfaces used for soot combustion in particulate diesel filters. To this end we have considered various species adsorbed and coadsorbed on the CeO_2(1 1 1) stoichiometric and reduced surface: O_2 molecules, small carbon clusters, isolated Ag atoms and small Ag_5 clusters. The results show that carbonaceous adsorbed species react with the ceria surface with formation of oxygenated carbon fragments and consequent formation of reduced ceria. The reaction is thermodynamically accessible as it involves only small energy costs. This result agrees with the experimental observation that the soot oxidation involves lattice and not ambient oxygen. Less clear is the mechanism which occurs to replenish the oxygen content of the oxide catalyst. In fact, both peroxo and superoxo species can form on the surface (these latters most likely in correspondence of low-coordinated Ce ions) but it remains unclear how these species re-establish the oxygen content. Probably by migration of oxygen vacancies from the bulk to the surface, an aspect which has not been considered here.

Since recent experimental studies point towards a beneficial effect of catalysts based on both Ag and CeO_2 components, we have considered how small silver units, atoms or clusters, deposited on the surface of ceria can modify its properties. We found that Ag atoms act as donor species which become oxidized and donate the valence electron to the oxide with formation of reduced Ce^{3+} ions. However, a charge transfer in the opposite direction occurs when the Ag atoms are stabilized (strongly) at O vacancies. In the first case, oxidized Ag atom on stoichiometric ceria, we notice a stronger bonding to the Ag^+ ion of gas-phase O_2 molecules, a result which suggests that the sticking probability of oxygen should increase in the presence of adsorbed Ag ions, facilitating oxygen refilling. On the contrary, no beneficial effect is found for an Ag atom adsorbed on a O vacancy since the final result is that the O_2 molecule fills the vacancy with formation of a peroxo group; the Ag atom is displaced from its original position, showing that the affinity of the vacancy for oxygen is much larger than for Ag.

Finally, we have considered Ag_5 clusters deposited on the stoichiometric and reduced ceria surfaces. In the first case the cluster behaves as the isolated atom, acting as one-electron donor. The situation is less clear when Ag_5 binds to an O vacancy since in this case some Ag atoms are in positive and some in neutral charge state. O_2 adsorption on this latter complex results in the formation of a superoxo species, an effect which has not been observed with other models considered in this study. This could indicate that at the interface between the Ag phase and reduced ceria samples one can form more easily activated oxygen species. However, the superoxo molecule can migrate below the Ag cluster and bind directly to the O vacancy with formation of a peroxo group. In this respect, the final effect is not very different from what occurs when O_2 binds directly to an O vacancy and the role of the silver particle is not particularly relevant, at least from a thermodynamic point of view. What has not been investigated here, and could be the subject of future studies, is the role of silver in the kinetics of the process and in reducing activation barriers for oxygen activation.

Acknowledgements

Gloria Preda thanks the Consortium CORIMAV between Pirelli and the University of Milano Bicocca for a PhD fellowship. Stimulating discussions with Livia Giordano and Luca Castellani are gratefully acknowledged. Finally, We thank Regione Lombardia and CILEA Consortium through a LISA Initiative (Laboratory for Interdisciplinary Advanced Simulation) for a CPU grant.

References

[1] D. Fino, V. Specchia, Powder Technol. 180 (2008) 64.
[2] E. Saab, E. Abi-Aad, M.N. Bokova, E.A. Zhilinskaya, A. Aboukais, Carbon 45 (2007) 561.
[3] M. Issa, C. Petit, A. Brillare, J.-F. Brilhac, Fuel 87 (2008) 740.
[4] A. Aboukais, E.A. Zhilinskaya, J.-F. Lamonier, I.N. Filiminaov, Colloids Surf. A: Physicochem. Eng. Aspects 260 (2005) 199.
[5] A. Bueno-Lopez, K. Krishna, B. van der Linden, G. Mul, J.A. Moulijn, M. Makkee, Catal. Today 121 (2007) 237.
[6] A. Bueno-Lopez, K. Krishna, M. Makkee, J.A. Moulijn, J. Catal. 230 (2005) 237.
[7] K. Krishna, A. Bueno-Lopez, M. Makkee, J.A. Moulijn, Appl. Catal. B: Environ. 75 (2007) 210.
[8] E. Aneggi, C. de Leitenburg, G. Dolcetti, A. Trovatelli, Catal. Today 114 (2006) 40.
[9] J. Liu, Z. Zhao, J. Wang, C. Xu, A. Duan, G. Jiang, Q. Yang, Appl. Catal. B: Environ. 84 (2008) 185.
[10] K. Krishna, A. Bueno-Lopez, M. Makkee, J.A. Moulijn, Appl. Catal. B: Environ. 75 (2007) 189.
[11] G. Avgouropoulos, M. Manzoli, F. Boccuzzi, T. Tabakova, J. Papavasiliou, T. Ioannides, V. Idakiev, J. Catal. 256 (2008) 237.
[12] A.J. Dyakonov, C.A. Little, Appl. Catal. B: Environ. 67 (2006) 52.
[13] J. Soria, A. Martinez-Arias, J. Conesa, J. Chem. Soc. Faraday Trans. 91 (1995) 1669.
[14] A. Martinez-Arias, J. Conesa, J. Soria, Res. Chem. Intermed. 33 (2007) 775.
[15] V.V. Pushkarev, V.I. Kovalchuk, J.L. d'Itri, J. Phys. Chem. B 108 (2004) 5341.
[16] Y.M. Choi, H. Abernathy, H.-T. Chen, M.C. Lin, M. Liu, ChemPhysChem 7 (2006) 1957.
[17] J. Guzman, S. Carrettin, A. Corma, J. Am. Chem. Soc. 127 (2005) 3286.
[18] N.V. Skorodumova, S.I. Simak, B.I. Lundqvist, I.A. Abrikosov, B. Johansson, Phys. Rev. Lett. 16 (2002) 166601.
[19] M. Nolan, S. Grigoleit, D.C. Sayle, S.C. Parker, G.W. Watson, Surf. Sci. 576 (2005) 217.
[20] P.J. Hay, R.L. Martin, J. Uddin, G.E. Scuseria, J. Chem. Phys. 125 (2006) 034712.
[21] D. Mei, N. Aaron Deskins, M. Dupuis, Q. Ge, J. Phys. Chem. C 111 (2007) 10514.
[22] M.M. Branda, C. Loschen, K. Neyman, F. Illas, J. Phys. Chem. C 112 (2008) 17643.
[23] C. Loschen, A. Migani, S.T. Bromley, F. Illas, K.M. Neyman, Phys. Chem. Chem. Phys. 10 (2008) 5730.
[24] M.B. Watkins, A.S. Foseter, A.L. Shluger, J. Phys. Chem. C 111 (2009) 15337.
[25] F. Esch, S. Fabris, L. Zhou, T. Montini, C. Africh, P. Fornasiero, G. Pomelli, R. Rosei, Science 309 (2005) 752.
[26] S. Fabris, G. Vicario, G. Calducci, S. de Gironcoli, S. Baroni, J. Phys. Chem. B 109 (2005) 22860.
[27] J.L.F. Da Silva, M.V. Ganduglia-Pirovano, J. Sauer, Phys. Rev. B 75 (2007) 045121.
[28] C. Loschen, J. Carrasco, K.M. Neyman, F. Illas, Phys. Rev. B 75 (2007) 035115.
[29] M.V. Ganduglia-Pirovano, A. Hofmann, J. Sauer, Surf. Sci. Rep. 62 (2007) 219.
[30] G. Pacchioni, J. Chem. Phys. 128 (2008) 182505.
[31] M.M. Branda, N.J. Castellani, R. Grau-Crespo, N.H. de Leeuw, N.C. Hernandez, J.F. Sanz, K.M. Neyman, F. Illas, J. Chem. Phys. 131 (2009) 094702.
[32] G. Kresse, J. Hafner, Phys. Rev. B 47 (1993) 558.
[33] G. Kresse, J. Furthmüller, Phys. Rev. B 54 (1996) 11169.
[34] P.E. Blöchl, Phys. Rev. B 50 (1994) 17953.
[35] V.I. Anisimov, F. Aryasetiawan, A.I. Lichtenstein, J. Phys.: Condens. Matter 9 (1997) 767.
[36] V.I. Anisimov, I.V. Solovyev, M.A. Korotin, M.T. Czyzyk, G.A. Sawatzky, Phys. Rev. B 48 (1993) 16929.
[37] I.V. Solovyev, P.H. Dederichs, V.I. Anisimov, Phys. Rev. B 50 (1994) 16861.
[38] S.H. Vosko, L. Wilk, M. Nusair, Can. J. Phys. 58 (1980) 1200.
[39] J.P. Perdew, J.A. Chevary, S.H. Vosko, K.A. Jackson, M.R. Pederson, D.J. Singh, C. Fiolhais, Phys. Rev. B 46 (1992) 6671.
[40] J.P. Perdew, J.A. Chevary, S.H. Vosko, K.A. Jackson, M.R. Pederson, D.J. Singh, C. Fiolhais, Phys. Rev. B 48 (1993) 4978.
[41] S.L. Dudarev, G.A. Botton, S.Y. Savrasov, C.J. Humphreys, A.P. Sutton, Phys. Rev. B 57 (1998) 1505.
[42] H.J. Monkhorst, J.D. Pack, Phys. Rev. B 13 (1976) 5188.
[43] M. Methfessel, A.T. Paxton, Phys. Rev. B 40 (1989) 3616.
[44] R.F.W. Bader, Atoms in Molecules, Oxford University Press, Oxford, 1990.
[45] (a) G. Henkelman, A. Arnaldsson, H. Jónsson, Comput. Mater. Sci. 36 (2006) 254–360;
(b) W. Tang, E. Sanville, G. Henkelman, J. Phys.: Condens. Matter 21 (2009) 084204.
[46] E. Wuilloud, B. Delley, W.-D. Schneider, Y. Baer, Phys. Rev. Lett. 53 (1984) 202.
[47] M.V. Ganduglia-Pirovano, J.L.F. Da Silva, J. Sauer, Phys. Rev. Lett. 102 (2009) 026101.
[48] H.-Y. Li, H.-F. Wang, X.-Q. Gong, Y.-L. Guo, G. Lu, P. Hu, Phys. Rev. B 79 (2009) 193401.
[49] H.L. Tuller, A.S. Nowick, J. Phys. Chem. Solids 38 (1977) 859.
[50] M. Huang, S. Fabris, Phys. Rev. B 75 (2007), 081404(R).
[51] H.-T. Chen, J.G. Chang, H.L. Chen, S.-P. Lu, J. Comput. Chem. 30 (2009) 2433.
[52] J.C. Conesa, Catal. Today 143 (2009) 315.
[53] A.L. Linsebigler, G. Lu, J.T. Yates, Chem. Rev. 95 (1995) 735.
[54] T. Berger, M. Sterrer, O. Diwald, E. Knözinger, D. Panayotov, T.L. Thompson, J.T. Yates, J. Phys. Chem. B 109 (2005) 6061.
[55] G. Preda, A. Migani, K.M. Neyman, S.T. Bromley, F. Illas, G. Pacchioni, J. Phys. Chem. C 115 (2011) 5817.
[56] J. Xu, J. Harmer, G. Li, T. Chapman, P. Collier, S. Longworth, S.C. Tsang, Chem. Commun. 46 (2010) 1887.
[57] G. Pacchioni, J. Koutecky, J. Chem. Phys. 88 (1988) 1066.
[58] M. Machida, Y. Murata, K. Kishikawa, D. Zhang, K. Ikeue, Chem. Mater. 20 (2008) 4489.
[59] D.A. Outka, J. Stöhr, W. Jark, P. Stevens, J. Solomon, E.J. Madix, Phys. Rev. B 35 (1987) 4119.
[60] P.A. Gravil, D.M. Bird, J.A. White, Phys. Rev. Lett. 77 (1996) 3933.
[61] E. Aneggi, J. Llorca, C. de Leitenburg, G. Dolcetti, A. Trovatelli, Appl. Catal. B: Environ. 91 (2009) 489.
[62] L.L. Murriel, R.T. Carlin, J. Catal. 159 (1996) 479.
[63] A.A. Herzing, C.J. Kiely, A.F. Carley, P. Landon, G.J. Hutchings, Science 321 (2008) 1331.
[64] V. Shapovalov, H. Metiu, J. Catal. 245 (2007) 205.
[65] M.M. Branda, N.C. Hernandez, J.F. Sanz, F. Illas, J. Phys. Chem. C 114 (2010) 1934.